

## A reassessment of HO<sub>x</sub> South Pole chemistry based on observations recorded during ISCAT 2000

G. Chen<sup>a,b,\*</sup>, D. Davis<sup>a</sup>, J. Crawford<sup>b</sup>, L.M. Hutterli<sup>c</sup>, L.G. Huey<sup>a</sup>, D. Slusher<sup>a</sup>, L. Mauldin<sup>d</sup>, F. Eisele<sup>d</sup>, D. Tanner<sup>a</sup>, J. Dibb<sup>e</sup>, M. Buhr<sup>a</sup>, J. McConnell<sup>f</sup>, B. Lefer<sup>c</sup>, R. Shetter<sup>c</sup>, D. Blake<sup>g</sup>, C.H. Song, K. Lombardi<sup>a</sup>, J. Arnoldy<sup>a</sup>

<sup>a</sup> School of Earth and Atmospheric Sciences, Georgia Institute of Technology, Atlanta, GA, USA

<sup>b</sup> NASA Langley Research Center, Hampton, VA, USA

<sup>c</sup> Department of Hydrology & Water Resources, University of Arizona, Tucson, AZ, USA

<sup>d</sup> Atmospheric Chemistry Division, National Center for Atmospheric Research, Boulder, CO, USA

<sup>e</sup> Climate Change Research Center, Institute for the Study of Earth, Ocean, and Space, University of New Hampshire, Durham, USA

<sup>f</sup> Division of Hydrologic Sciences, Desert Research Institute, Reno, NV, USA

<sup>g</sup> Department of Chemistry, University of California, Irvine, CA, USA

Received 3 October 2002; accepted 7 July 2003

### Abstract

Reported here are modeling results based on ISCAT (Investigation of Sulfur Chemistry of Antarctic Troposphere) 2000 observations recorded at the South Pole (SP) during the Austral Summer of 2000. The observations included a comprehensive set of photochemical parameters, e.g., NO, O<sub>3</sub>, and CO. It is worthy to note that not only were OH and HO<sub>2</sub> observed, but also HO<sub>x</sub> precursor species CH<sub>2</sub>O, H<sub>2</sub>O<sub>2</sub>, and HONO were measured. Previous studies have suggested that HONO is the major source of OH/HO<sub>x</sub> in the Arctic; however, observed HONO levels at SP induced dramatic model overprediction of both HO<sub>x</sub> and NO<sub>x</sub> when used to constrain the model calculations. In contrast, model predictions constrained by observed values of CH<sub>2</sub>O and H<sub>2</sub>O<sub>2</sub> are consistent with the observations of OH and HO<sub>2</sub> (i.e., within 20%) for more than half of the data. Significant model overpredictions of OH, however, were seen at the NO levels lower than 50 pptv or higher than 150 pptv. An analysis of HO<sub>x</sub> budget at the median NO level suggests that snow emissions of H<sub>2</sub>O<sub>2</sub> and CH<sub>2</sub>O are the single most important primary source of SP HO<sub>x</sub>, contributing 46% to the total source. Major sinks for HO<sub>x</sub> are found to be dry deposition of HO<sub>2</sub>NO<sub>2</sub> and HNO<sub>3</sub> as well as their reactions with OH. Although ISCAT 2000 led to a major progress in our understanding of SP HO<sub>x</sub> chemistry, critical aspects of this chemistry are still in need of further investigation.

© 2004 Elsevier Ltd. All rights reserved.

**Keywords:** Antarctica; South Pole; Photochemistry; HO<sub>x</sub>; Snow emissions; ISCAT

### 1. Introduction

It has long been recognized that free radicals are responsible for the tropospheric oxidation of most

reduced trace gases emitted from natural as well as anthropogenic sources (e.g., Levy, 1974; Logan et al., 1981; Chameides and Davis, 1982; Thompson, 1992). Among the more important of these is the hydroxyl radical (OH). It largely controls the oxidizing power of the atmosphere. Yet another is the hydroperoxyl radical (HO<sub>2</sub>), a product of many OH reactions. In the presence of nitric oxide (NO), rapid cycling between OH and HO<sub>2</sub>

\*Corresponding author. NASA Langley Research Center, Hampton, VA, USA.

E-mail address: gao.chen-1@nasa.gov (G. Chen).

can enhance atmospheric OH through secondary production strengthening its dominance as the major tropospheric oxidizing agent. Because of this tight chemical linkage, the sum of HO<sub>2</sub> and OH is frequently abbreviated as HO<sub>x</sub>. Studies focused on tropospheric HO<sub>x</sub> sources and sinks are numerous and define one of the most important aspects of atmospheric chemistry (e.g., Crawford et al., 1999; Chen et al., 2001a, b; Jaegle et al., 2000,2001; Olson et al., 2001; Tan et al., 1998, 2001; Wang et al., 2001).

Our present understanding of HO<sub>x</sub> chemistry indicates that at low altitudes production of HO<sub>x</sub> is often proportional to UV solar radiation and H<sub>2</sub>O levels. This naturally leads to an expected strong latitudinal gradient in OH. For example, both model results and field observations reveal that the tropics have some of the highest OH values to be found (e.g., Logan et al., 1981; Chamedies and Tan, 1981; Mauldin et al., 1999). For this reason, it was with great surprise that the first South Pole (SP) observations revealed OH levels whose summertime 24 h average was within 10% of the corresponding value in the tropics (Mauldin et al., 2001). Concomitant with these elevated OH levels were extraordinarily high mixing ratios (median, 225 pptv) of NO (Davis et al., 2001). These authors presented strong evidence suggesting the source of this SP NO being emissions from the snowpack, a by-product from the photolysis of nitrate. A modeling analysis of these ISCAT 1998 (Investigation of Sulfur Chemistry in Antarctic Troposphere) data by Chen et al. (2001b) showed that OH levels were a strong non-linear function of NO. The dominant source of OH was the recycling of HO<sub>x</sub> through the reaction sequence HO<sub>2</sub> + NO → OH + NO<sub>2</sub>, followed by OH + CO(O<sub>2</sub>) → HO<sub>2</sub> + CO<sub>2</sub> (e.g., see Table 1 [R4] and [R3]). It was further shown that the largest primary source of HO<sub>2</sub> was photolysis of CH<sub>2</sub>O [R13], the latter being a product from the OH initiated oxidation of CH<sub>4</sub> [R10]. Due to the high NO levels the amplification of HO<sub>x</sub> through CH<sub>4</sub> oxidation was nearly a factor of 1.5 (i.e., HO<sub>2</sub> produced per OH consumed). The oxidation of CH<sub>4</sub>, therefore, serves as a net source of HO<sub>x</sub>, rather than a net sink as is typical of most remote boundary layer (BL) settings.

While the observed trends in NO, H<sub>2</sub>O, O<sub>3</sub>, and UV irradiance appeared to explain a large fraction of the ISCAT 1998 OH observations, a more detailed comparison of model predictions against observations exposed some shortcomings. Among these was the underprediction of OH at certain times. This has suggested the possibility of additional HO<sub>x</sub> sources. Based on several Arctic studies, the additional sources were speculated to be the result of snowpack emissions of H<sub>2</sub>O<sub>2</sub>, CH<sub>2</sub>O, and/or HONO (e.g., Dibb et al., 2002; Hutterli et al., 1999, 2001; McConnell et al., 1997; Sumner and Shepson, 1999; Zhou et al., 2001). Sensitivity tests by Chen et al. (2001b) showed that the photolysis of only

Table 1  
Summary of important photochemical reactions for SP HO<sub>x</sub>

R1	O <sub>3</sub> + <i>hν</i> → O ( <sup>1</sup> D) + O <sub>2</sub>
R2	O ( <sup>1</sup> D) + H <sub>2</sub> O → OH + OH
R3	OH + CO (O <sub>2</sub> ) → HO <sub>2</sub> + CO <sub>2</sub>
R4	HO <sub>2</sub> + NO → OH + NO <sub>2</sub>
R5	HO <sub>2</sub> + HO <sub>2</sub> → H <sub>2</sub> O <sub>2</sub>
R6	H <sub>2</sub> O <sub>2</sub> + <i>hν</i> → OH + OH
R7	H <sub>2</sub> O <sub>2</sub> + OH → HO <sub>2</sub> + H <sub>2</sub> O
R8	H <sub>2</sub> O <sub>2</sub> → RO/AS/DD <sup>a</sup>
R9	OH + HO <sub>2</sub> → H <sub>2</sub> O + O <sub>2</sub>
R10	OH + CH <sub>4</sub> (O <sub>2</sub> ) → CH <sub>3</sub> O <sub>2</sub> + H <sub>2</sub> O
R11	CH <sub>3</sub> O <sub>2</sub> + NO (O <sub>2</sub> ) → HO <sub>2</sub> + CH <sub>2</sub> O + NO <sub>2</sub>
R12	CH <sub>2</sub> O + <i>hν</i> → H <sub>2</sub> + CO
R13	CH <sub>2</sub> O + <i>hν</i> (2O <sub>2</sub> ) → 2HO <sub>2</sub> + HO <sub>2</sub> + CO
R14	CH <sub>2</sub> O + OH + O <sub>2</sub> → HO <sub>2</sub> + H <sub>2</sub> O + CO
R15	CH <sub>2</sub> O → RO/AS/DD
R16	OH + NO → HONO
R17	HONO + <i>hν</i> → OH + NO
R18	OH + HONO → NO <sub>2</sub> + H <sub>2</sub> O
R19	HONO → RO/AS/DD
R20	OH + NO <sub>2</sub> → HNO <sub>3</sub>
R21	HNO <sub>3</sub> + <i>hν</i> → OH + NO <sub>2</sub>
R22	OH + HNO <sub>3</sub> → NO <sub>3</sub> + H <sub>2</sub> O
R23	HNO <sub>3</sub> → RO/AS/DD
R24	HO <sub>2</sub> + NO <sub>2</sub> → HO <sub>2</sub> NO <sub>2</sub>
R25	HO <sub>2</sub> NO <sub>2</sub> + M → HO <sub>2</sub> + NO <sub>2</sub> + M
R26	HO <sub>2</sub> NO <sub>2</sub> + <i>hν</i> → HO <sub>2</sub> + NO <sub>2</sub>
R27	HO <sub>2</sub> NO <sub>2</sub> + <i>hν</i> → OH + NO <sub>3</sub>
R28	HO <sub>2</sub> NO <sub>2</sub> + OH → H <sub>2</sub> O + NO + O <sub>2</sub>
R29	HO <sub>2</sub> NO <sub>2</sub> → RO/AS/DD

<sup>a</sup> RO = Rainout; AS = Aerosol scavenging; DD = Dry deposition.

very modest emissions of any of the above species could have provided the necessary primary source of HO<sub>x</sub>. However, it was not possible to quantify these potential sources since no measurements were made.

From Chen et al.'s (2001b) analysis, it was also shown that the major HO<sub>x</sub> loss pathways at SP are reactions of OH and HO<sub>2</sub> with NO<sub>2</sub> to form HNO<sub>3</sub> and HO<sub>2</sub>NO<sub>2</sub>. The final step in the loss process was speculated to involve mainly dry deposition of these acidic species (see Table 1, [R23] and [R29]) as well as, to a much lesser extent, reactions with OH ([R22] and [R28]); however, this was not confirmed since only very limited measurements of HNO<sub>3</sub> and none for HO<sub>2</sub>NO<sub>2</sub> were obtained during the first ISCAT study.

ISCAT 2000 was carried out at Amundsen-Scott SP station, Antarctica during the months of November and December 2000. Quite significant in ISCAT 2000 though were the additional measurements of HO<sub>2</sub>, H<sub>2</sub>O<sub>2</sub>, CH<sub>2</sub>O, HONO, and HO<sub>2</sub>NO<sub>2</sub>. As a result, this paper has focused on re-examining current photochemical mechanisms applicable to the SP mixed layer, particularly the processes controlling the levels of HO<sub>x</sub>.

## 2. Model descriptions

The model used in this study is the same as that employed in the ISCAT 1998 analysis. It is a time dependent box model containing explicit  $\text{HO}_x$ - $\text{NO}_x$ - $\text{CH}_4$  chemistry (71 reactions) and parameterized NMHC chemistry (184 reactions). The latter chemistry has been significantly modified from the CAL scheme reported by Lurmann et al. (1986) (see e.g., Crawford et al., 1999). Typical model inputs consist of  $\text{NO}$ ,  $\text{CO}$ ,  $\text{O}_3$ ,  $\text{H}_2\text{O}$ , ambient temperature, and pressure. However, the model can also accommodate observational constraints based on measurements of  $\text{OH}$ ,  $\text{HO}_2$ ,  $\text{HNO}_3$ ,  $\text{HO}_2\text{NO}_2$ ,  $\text{H}_2\text{O}_2$ ,  $\text{CH}_2\text{O}$ , and  $\text{HONO}$ . The photolysis coefficients used in the analysis are those derived from in situ actinic flux measurements (see Davis et al., 2004a). Since no diurnal UV flux variations occur at SP during the Austral summer (there are variations, however, due to shifts in the overhead  $\text{O}_3$  column density), photochemical steady state was assumed for all model calculated species. As the lifetimes of  $\text{HO}_x$  species are quite short, i.e.,  $\sim 3$  s for  $\text{OH}$  and  $\sim 30$ – $80$  s for  $\text{HO}_2$ , this assumption is quite reasonable for both species. The first order rate for heterogeneous removal of soluble species was taken to be  $9 \times 10^{-5} \text{ s}^{-1}$ , the best deposition loss rate estimate for  $\text{HNO}_3$  and  $\text{HO}_2\text{NO}_2$  by Slusher et al. (2002) based on ISCAT 2000 dataset. This value is about one order of magnitude higher than that used in the 1998 study, and is based on the 2000 measurements of  $\text{HNO}_3$ . If the current deposition loss rate were applied to the ISCAT 98 analysis, the model  $\text{OH}$  would decrease, on average, by nearly a factor of 1.5 and the median  $P(\text{O}_3)$  would be reduced by  $\sim 0.8$  ppbv  $\text{day}^{-1}$ . Model uncertainty based solely on rate coefficient uncertainties has been evaluated based on Monte Carlo sensitivity calculations. The model  $\text{HO}_x$  uncertainty based on these calculations was estimated at 40%.

## 3. Results and discussion

A summary of the observational data recorded during ISCAT 2000, together with a description of the instrumental technique (e.g., sensitivity and calibration), are presented in Davis and Eisele, 2004. For further details concerning a specific measurement, the reader is encouraged to examine individual contributions to this special issue. For completeness, however, the typical total uncertainty (random plus systematic errors) assigned to observations of  $\text{OH}$ ,  $\text{HO}_2$ ,  $\text{HNO}_3$ , and  $\text{HO}_2\text{NO}_2$  were in the 20–60% range depending on the  $S/N$  (signal to noise) ratio of a specific measurement.

The interpretive analysis of ISCAT 2000  $\text{HO}_x$  observations was based on 4604 individual model runs. These runs were mostly derived from 10-min data averages of the observed parameters  $\text{NO}$ ,  $\text{O}_3$ ,  $\text{H}_2\text{O}$ ,

and several  $j$  values. In addition, values for  $\text{CO}$  and nonmethane hydrocarbons (NMHC) were interpolated from grab sample observations having a typical temporal resolution of 2 to 4 samples  $\text{day}^{-1}$ . (The authors note that the day-to-day variations in  $\text{CO}$  were typically less than 5% and NMHC levels were sufficiently low as to have a negligible effect on the  $\text{HO}_x$  results.) Among the 4604 model runs completed, 2455 of these had  $\text{OH}$  measurements and 199 had  $\text{HO}_2$  data. However, coincident  $\text{OH}$  and  $\text{HO}_2$  data were not available because the same instrument was used to measure both species such that these measurements could not be made simultaneously. In addition to the  $\text{HO}_x$  measurements, there were 754 and 1185 runs having measurements of  $\text{CH}_2\text{O}$  and  $\text{H}_2\text{O}_2$ , respectively. Both  $\text{CH}_2\text{O}$  and  $\text{H}_2\text{O}_2$  observations were recorded at 1 m above the snow surface (Hutterli et al., 2004). The measurement of  $\text{HONO}$  was made near the surface and at 10 m above the surface (Dibb et al., 2004). However, only very limited observations were recorded at 10 m. It was this group of data at 10 m that was used to constrain the model for purposes of evaluating the impact of  $\text{HONO}$  on SP  $\text{HO}_x$  sources. Other than  $\text{H}_2\text{O}_2$ ,  $\text{CH}_2\text{O}$ , and  $\text{HONO}$ , all data were collected at 10 m above the snow surface. Since the vertical mixing is typically weak in SP (Onclay et al., 2004), the  $\text{H}_2\text{O}_2$  and  $\text{CH}_2\text{O}$  levels may be lower at 10 m. Estimates of the eddy-diffusion calculation indicate that for neutral conditions this minor difference in sampling heights could lead to 7% and 5% drops for  $\text{H}_2\text{O}_2$  and  $\text{CH}_2\text{O}$ , respectively (also see Hutterli et al., 2004). One should expect larger drops for stable conditions, which is probably more prevalent in SP. This will be further examined in terms of their impact on  $\text{HO}_x$  later in the text. As related to the  $\text{HO}_2$  observations, only the sum of the concentrations of  $\text{HO}_2$ ,  $\text{OH}$ ,  $\text{CH}_3\text{O}_2$ , and  $\text{RO}_2$  (Mauldin et al., 2004) could be measured as the instrument was configured at SP. The  $\text{HO}_2$  fraction of the total radical sum was estimated from model runs. The  $\text{HO}_2$  fraction typically ranged from 69% to 78%, with a median of 75%.

### 3.1. Comparison of model results with observations

As stated earlier, a major goal of this study was to quantitatively re-evaluate sources and sinks of SP mixed layer  $\text{HO}_x$  under summertime conditions. In particular, this required our examining the magnitude of the  $\text{HO}_x$  source resulting from snow emissions of  $\text{H}_2\text{O}_2$ ,  $\text{CH}_2\text{O}$ , and  $\text{HONO}$ . During ISCAT 2000, snow emissions significantly enhanced the measured levels of all these  $\text{HO}_x$  precursors (Dibb et al., 2004; Hutterli et al., 2004). Our standard model (gas phase chemistry only) can only predict less than 4%, 39%, and 5% of observed levels of  $\text{H}_2\text{O}_2$ ,  $\text{CH}_2\text{O}$ , and  $\text{HONO}$ , respectively. Thus, assessing the effect of snow emission on SP  $\text{HO}_x$  levels requires model calculations constrained by the observed values of

these precursor species. The effect of snow emissions then can be estimated by comparing the constrained model results with those from the standard model. Finally, the results from both models are compared against the observations.

Fig. 1a shows observed OH values and model results from the standard model. Fig. 1a shows that both modeled and observed OH are strongly modulated by NO with peak values occurring at  $\sim 100$  pptv of NO. It is also apparent that model values are generally lower, except for values of NO  $< 40$  pptv. Overall, the median ratio of model to observation ( $M/O$ ) is 0.68. Following the same approach for HO<sub>2</sub>, Fig. 1b shows that observed HO<sub>2</sub> values are also higher than those predicted by the model. (The smaller range of NO values plotted against HO<sub>2</sub> versus OH primarily reflects the limited number of ISCAT 2000 HO<sub>2</sub> observations.) Again, the median  $M/O$  ratio for HO<sub>2</sub> is about 0.65. These differences between

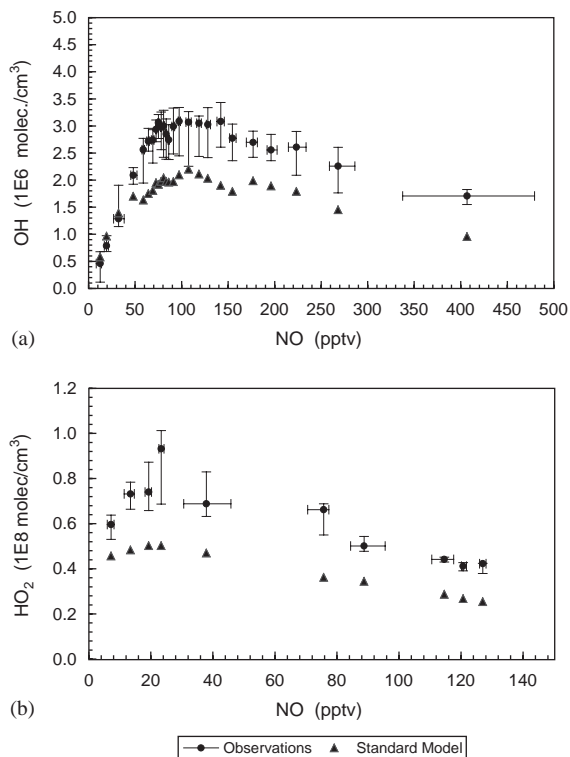


Fig. 1. Comparison of observations with standard model predictions for: (a) OH and (b) HO<sub>2</sub> as a function of NO. Each point in panel (a) represents the binned results from individual model runs or the average value from 10 min of observation. In each case 100 values have been used. In panel (b), each data point represents the binned results from only 20 values. Final values plotted are median values and the error bars indicate the lower and upper quartiles on the observational data. Standard model refers to the model with gas phase chemistry only.

model and observations appear to be modest in comparison with model and observation uncertainties of 40%, which suggests that the median model bias could be removed by significant shifts in some kinetic rate coefficients and/or HO<sub>x</sub> measurement calibration factors. Alternatively, the model underprediction of HO<sub>x</sub> could also indicate that the model either underestimates HO<sub>x</sub> sources or overestimates its sinks.

To test the hypothesis that HO<sub>x</sub> sources might be underestimated, the ISCAT 2000 observations of CH<sub>2</sub>O, H<sub>2</sub>O<sub>2</sub>, and HONO were used to constrain the model. All three species have previously been identified at Arctic sites. In each case, it has been stated that the major sources of these species were emissions from the snowpack (e.g., Dibb et al., 2002; Hutterli et al., 1999, 2001; McConnell et al., 1997; Sumner and Shepson, 1999; Zhou et al., 2001). Fig. 2 shows HO<sub>x</sub> from both observations and model calculations constrained by observed values of CH<sub>2</sub>O, H<sub>2</sub>O<sub>2</sub>, and HONO. Two different constraint levels are shown here. At the first level, only CH<sub>2</sub>O and H<sub>2</sub>O<sub>2</sub> observations are used to constrain the model. At the second constraint level, all three species (CH<sub>2</sub>O, H<sub>2</sub>O<sub>2</sub>, and HONO) are used to

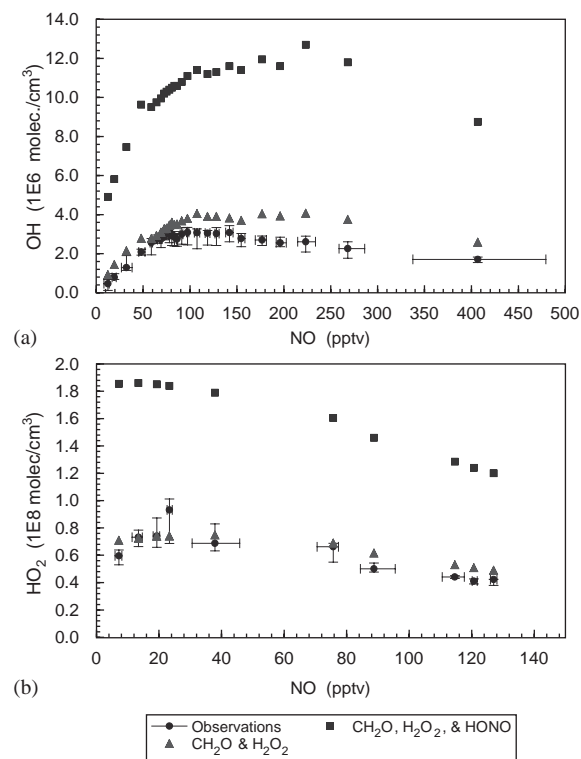


Fig. 2. Comparison of observations with constrained model predictions for: (a) OH and (b) HO<sub>2</sub> as a function of NO. Model and observational values have been derived in the same way as cited for Fig. 1.

constrain the model. It can be seen in the figures that constraining all three precursors leads to significant model overestimation of both OH and HO<sub>2</sub>. The model values are factors of 2 to 3 and factors of 3 to 5 higher than observations of HO<sub>2</sub> and OH, respectively. At the median NO level of 89 pptv, the model predicted OH concentration approaches to  $1.1 \times 10^7$  molec cm<sup>-3</sup>.

Although direct measurements of OH have not been conducted at any Arctic sites, model estimates of OH based on HONO measurements are available for Summit, Greenland and Alert, Canada. It should first be noted, however, that the average SP HONO level is about a factor of 3–4 higher than that of Summit and a factor of 6 higher than the value measured at 5 m above surface in Alert. For springtime conditions at Alert, Zhou et al. (2001) suggested that production from HONO would increase peak OH values (noon) to  $1.1 \times 10^6$  molec cm<sup>-3</sup>. Based on observations at Summit, Yang et al. (2002) predicted noontime OH values approaching to  $9 \times 10^6$  molec cm<sup>-3</sup> in one case; however, the derived diel average was only  $\sim 4 \times 10^6$  molec cm<sup>-3</sup>. Although there are significant differences in the levels of other OH precursors between the SP and Arctic studies; the major factor driving the differences in model OH levels is most likely to be the in observed HONO levels.

In another assessment of the HONO observations, we examined the impact of HONO on the levels of NO<sub>x</sub>, the rationale being that HONO photolysis [R17] also serves as a source for NO. In fact, for periods of concurrent observation, NO values (at 10 m) and HONO values observed near the surface (85 cm) are positively correlated. This relationship can be well approximated by a second order polynomial with an *R*<sup>2</sup> value of 0.83. However, it is difficult to reconcile the observations of both of these species. For example, under the conditions of ISCAT 2000, the typical photochemical lifetime of HONO was only 7–10 min while that for NO<sub>x</sub> was 7–25 h. Taking the average lifetime for each species and the median value of HONO sampled at 10 m (i.e.,  $\sim 26$  pptv), the median NO<sub>x</sub> level is predicted to be  $\sim 10$  times higher than what was observed. This raises the question of whether the measurement of HONO might suffer from some systematic error (e.g., chemical interference), although one can not rule out the possibility that the model mechanism might miss major HO<sub>x</sub> and NO<sub>x</sub> loss processes unique to the polar troposphere. While the mist chamber technique has been used in numerous studies involving various environmental conditions, there still exists the possibility of interference from any species that readily dissolves in aqueous solution to make nitrite. At this point, there are major difficulties in interpreting the HONO observations. Thus, we have focused our attention on the impact from snow emissions of CH<sub>2</sub>O and H<sub>2</sub>O<sub>2</sub> in the text that follows.

### 3.2. HO<sub>x</sub> enhancement due to CH<sub>2</sub>O and H<sub>2</sub>O<sub>2</sub>

Fig. 2 shows model results from calculations constrained by observed CH<sub>2</sub>O and H<sub>2</sub>O<sub>2</sub> levels. The constrained model HO<sub>2</sub> values are much closer to observations, as shown in Fig. 2b, than those from standard model. The median *M/O* ratio is 1.12. In the case of OH, however, median *M/O* ratio is 1.27 (1.22 for NO < 130 pptv). Higher *M/O* ratios of  $\sim 1.5$  can be seen at NO values above 150 pptv. There are about 22% of model runs within this NO range. One of the contributing factors could be that the surface measurements of CH<sub>2</sub>O and H<sub>2</sub>O<sub>2</sub> could be too high for 10 m, the sampling height of OH and NO. Since there were no actual measurements available at 10 m, we have carried out sensitivity calculations with lowered the CH<sub>2</sub>O and H<sub>2</sub>O<sub>2</sub> by the estimated concentration drop (see discussions in Section 3) from 1 to 10 m. The corresponding decrease in *M/O* ratio for either OH or HO<sub>2</sub> is less than 3%. Since the larger model overestimations are at high NO levels and high NO levels are typically associated with meteorological stable conditions (Davis et al., 2004b), larger vertical gradient for both CH<sub>2</sub>O and H<sub>2</sub>O<sub>2</sub> can be expected for these conditions, which will, in turn, lead to greater reduction in *M/O* ratio. We do not believe, however, this difference in sampling heights will completely remove the model bias. Other explanations may involve one or a combination of factors, including missing HO<sub>x</sub> loss processes, systematic model uncertainty in rate coefficients, and potential bias in observations of CH<sub>2</sub>O, H<sub>2</sub>O<sub>2</sub>, and OH.

Despite the existing bias, constraining H<sub>2</sub>O<sub>2</sub> and CH<sub>2</sub>O does bring the model results closer to observations. In addition, it is necessary to constrain the model with observed CH<sub>2</sub>O and H<sub>2</sub>O<sub>2</sub> levels to better reflect the SP photochemical environmental conditions. As discussed earlier, Arctic studies have shown these two species to be important HO<sub>x</sub> sources. To better understand the impact from snow emitted CH<sub>2</sub>O and H<sub>2</sub>O<sub>2</sub> on SP HO<sub>x</sub>, here we present the results from a series of model sensitivity calculations to examine the HO<sub>x</sub> sensitivities to H<sub>2</sub>O<sub>2</sub> and CH<sub>2</sub>O as well as their dependence on NO levels. The 4604 original model runs were divided into three groups according to the NO values: (1) runs where NO levels were in the lower 25th percentile of the distribution (i.e., 67 pptv); (2) runs having NO values within the inner quartiles; and (3) runs having NO values larger than the 75th percentile (i.e., 123 pptv). Three representative model runs were generated from these three NO groups by taking appropriate median values for model input parameters. These runs were then used in evaluation of the sources of CH<sub>2</sub>O and H<sub>2</sub>O<sub>2</sub> and their effect on SP HO<sub>x</sub>.

Shown in Figs. 3a and b are the observed medians for H<sub>2</sub>O<sub>2</sub> and CH<sub>2</sub>O as well as predictions from the standard model which is based on gas phase chemistry

alone. Similar to other soluble species, the model assumes a dry deposition rate of  $9 \times 10^{-5} \text{ s}^{-1}$ . The flux measurements by Hutterli et al. (2004) indicate that the snow, on average, is a net source of atmospheric  $\text{H}_2\text{O}_2$  and  $\text{CH}_2\text{O}$ . But, it does not rule out dry deposition as a part of the air–snow exchange processes. The zero deposition case described by Hutterli et al. (2004) can be considered as a limiting case in which the emissions balance deposition. On average, the gas phase chemistry can only account for up to 3% and 30% of the observations of  $\text{H}_2\text{O}_2$  and  $\text{CH}_2\text{O}$ , respectively. Even if the dry deposition rate is one order of magnitude smaller, it still leaves more than 70% of  $\text{H}_2\text{O}_2$  and 30% of  $\text{CH}_2\text{O}$  observations unexplained. These results are consistent with those from a more detailed analysis by Hutterli et al. (2004). Together, the discrepancy between observations and model predictions based on gas phase chemistry alone argues that substantial amount of  $\text{H}_2\text{O}_2$  and  $\text{CH}_2\text{O}$  are sustained by snowpack emissions. This is supported by  $\text{CH}_2\text{O}$  air–snow transfer model predictions (Hutterli et al., 2002) and by direct  $\text{CH}_2\text{O}$  and  $\text{H}_2\text{O}_2$  flux measurements during ISCAT 2000. A comparison of those fluxes with the photochemical modeling can be found in Hutterli et al. (2004). Similar results were also reported by Hutterli et al. (1999, 2001) for analyses of  $\text{CH}_2\text{O}$  and  $\text{H}_2\text{O}_2$  observations recorded at Summit,

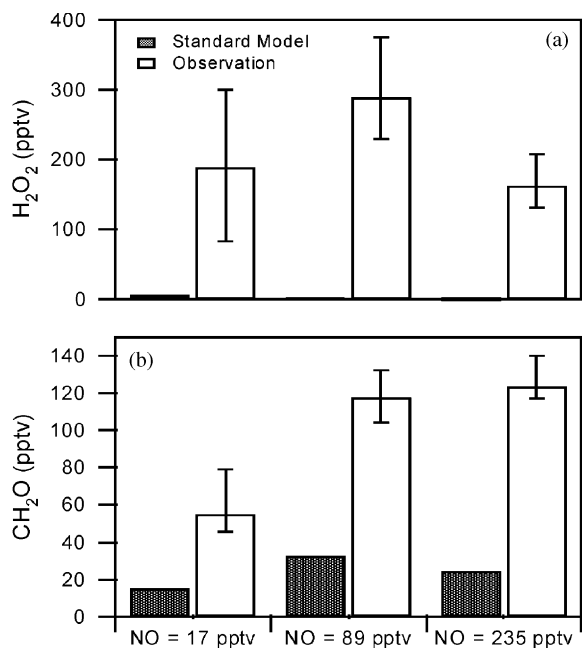


Fig. 3. Comparison of observations with standard model predictions for: (a)  $\text{H}_2\text{O}_2$  and (b)  $\text{CH}_2\text{O}$ . The model calculations are based on representative runs derived from three data groupings defined by the NO concentration ranges. The observational bars are median values and the error bars on these denote the upper and lower quartile levels.

Greenland and by Sumner et al. (2002) for a  $\text{CH}_2\text{O}$  study in Alert, Nunavut, Canada.

To better understand the role of snow emissions, it is important to quantify how each of these emitted species influences  $\text{HO}_x$  levels. As noted earlier, sensitivity calculations were based on median conditions for low, mid, and high NO levels. The results of the sensitivity calculations are summarized in Fig. 4. Shown here are the observed medians for OH and  $\text{HO}_2$ , as well as the model predicted concentrations for these species based on four different constraint levels. Level 1 constraint represents the standard model (i.e., not constrained by either  $\text{H}_2\text{O}_2$  or  $\text{CH}_2\text{O}$ ); level 2 is constrained by  $\text{H}_2\text{O}_2$  only; level 3 is constrained by  $\text{CH}_2\text{O}$  only; and level 4 shows the combined effects of being constrained by both  $\text{H}_2\text{O}_2$  and  $\text{CH}_2\text{O}$ . From Fig. 4a, model predicted increases in OH from  $\text{H}_2\text{O}_2$  only range from only 0.3 to  $1.0 \times 10^6 \text{ molec cm}^{-3}$  (32–58%), while the corresponding  $\text{HO}_2$  increase shown in Fig. 4b varies from 0.5 to  $1.5 \times 10^7 \text{ molec cm}^{-3}$  (28–60%). In the case of constraining  $\text{CH}_2\text{O}$  only, from the lowest NO case to highest case, the model predict OH increase varies from 0.2 to  $1.7 \times 10^6 \text{ molec cm}^{-3}$  (21–106%), while the corresponding  $\text{HO}_2$  enhancement ranges from 1.2 to

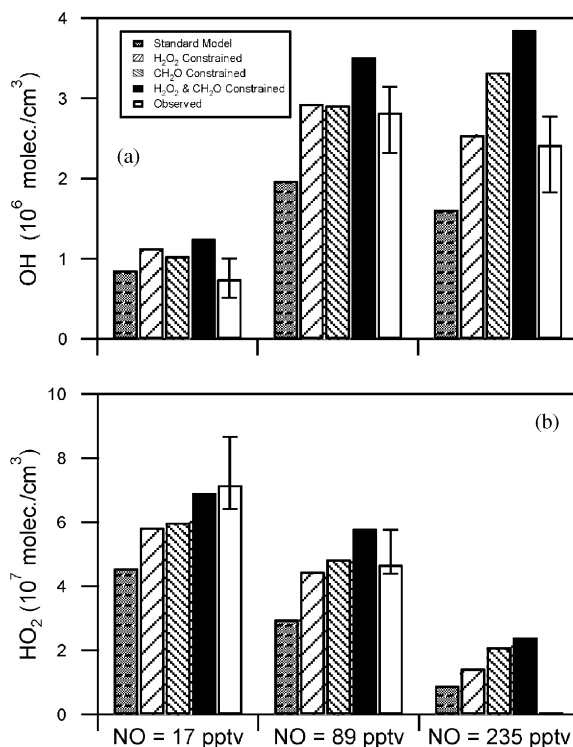


Fig. 4. Model estimated impact of snow emissions of  $\text{CH}_2\text{O}$  and  $\text{H}_2\text{O}$  on: (a) OH and (b)  $\text{HO}_2$  and comparison with observations. Observational values are median values derived from the corresponding NO groups. Observational error bars represent inner quartile values.

$1.9 \times 10^7 \text{ molec cm}^{-3}$  (31–134%). Considering that the observed levels of  $\text{H}_2\text{O}_2$  are much higher than that of  $\text{CH}_2\text{O}$ , one can conclude SP  $\text{HO}_x$  is much more responsive to  $\text{CH}_2\text{O}$  than to  $\text{H}_2\text{O}_2$  on a per-molecule basis. For example, the average OH sensitivities to  $\text{H}_2\text{O}_2$  and  $\text{CH}_2\text{O}$  are  $3.5 \times 10^3$  and  $8.3 \times 10^3 \text{ molec cm}^{-3} \text{ pptv}^{-1}$ , respectively. Even larger contrast can be seen in the case of  $\text{HO}_2$ , i.e., 0.5 vs.  $1.7 \times 10^5 \text{ molec cm}^{-3} \text{ pptv}^{-1}$ . A major reason for this is the difference in the photolysis rate for the two compounds. On average,  $\text{CH}_2\text{O}$  photolyzes nearly 5 times faster than for  $\text{H}_2\text{O}_2$ . Although not shown, the sensitivity calculations also reveal that the OH sensitivity is a strong function of NO, increasing by a factor of 4 from the lowest NO level to the highest as the partitioning of  $\text{HO}_x$  is shifted more favorably toward OH. Interestingly, the  $\text{HO}_2$  sensitivity has a reverse dependence on NO levels, decreasing by a factor of  $\sim 2.3$  from the highest NO to the lowest reflecting the decrease in  $\text{HO}_x$  lifetime with increasing NO levels.

When the model is constrained by both  $\text{H}_2\text{O}_2$  and  $\text{CH}_2\text{O}$ , the increase in OH and  $\text{HO}_2$  levels, on average, is 17% less than that which would be estimated from taking the simple sum of the increases calculated independently for  $\text{H}_2\text{O}_2$  and  $\text{CH}_2\text{O}$ . This 17% difference is partially due to the additional loss resulting from the reaction  $\text{OH} + \text{HO}_2$  ([R7] see Table 1). The contribution from this reaction obviously would rapidly increase with  $\text{HO}_x$  level itself in a quadratic form. For the mid NO level case, there is a factor of  $\sim 1.5$  increase in this loss when comparing model constrained by both  $\text{H}_2\text{O}_2$  and  $\text{CH}_2\text{O}$  with calculation constrained by only  $\text{H}_2\text{O}_2$  or  $\text{CH}_2\text{O}$ . In addition to the loss increase, another important factor is the decrease in the net effect of snow emission on  $\text{HO}_x$  because of the enhancement in  $\text{HO}_x$ . For example, the net contribution from  $\text{H}_2\text{O}_2$  to  $\text{HO}_x$  can be evaluated by Eq. (1):

$$P_{\text{H}_2\text{O}_2}(\text{HO}_x) = 2j_6[\text{H}_2\text{O}_2] - 2k_5[\text{HO}_2][\text{HO}_2], \quad (1)$$

where  $j_6$  and  $k$ 's are reaction rate coefficients. As shown in Eq. (1), for a given ambient concentration of  $\text{H}_2\text{O}_2$  its contribution to  $\text{HO}_x$  is a quadratic function of  $\text{HO}_x$  level. Again for mid NO levels,  $P_{\text{H}_2\text{O}_2}(\text{HO}_x)$  from the calculation constrained by both  $\text{CH}_2\text{O}$  and  $\text{H}_2\text{O}_2$  is less than 60% of the value if only  $\text{H}_2\text{O}_2$  is constrained. In the case of  $\text{CH}_2\text{O}$ , an equation similar to Eq. (1) can also be derived but is much more complicated due to the complexity of  $\text{CH}_4$  chemistry. The net effect of  $\text{CH}_2\text{O}$ , however, has a much weaker dependence on  $\text{HO}_x$  level. Again for mid level NO case, the decrease in  $\text{CH}_2\text{O}$  contribution is only about 25%.

### 3.3. $\text{HO}_x$ sinks

In Chen et al.'s. (2001b) 1998 ISCAT study, the authors suggested that the largest  $\text{HO}_x$  loss pathways

involve the formation of  $\text{HNO}_3$  and  $\text{HO}_2\text{NO}_2$ , i.e., reactions [R20] and [R24]. The role of  $\text{HO}_2\text{NO}_2$  can be seen in the sequence of reactions [R25], [R26], [R27], [R28] and [R29] as shown in Table 1. The net  $\text{HO}_x$  loss can be estimated from Eq. (2):

$$k_{24}[\text{HO}_2][\text{NO}_2] + k_{28}[\text{OH}][\text{HO}_2\text{NO}_2] - (k_{25} + j_{26} + j_{27})[\text{HO}_2\text{NO}_2]. \quad (2)$$

It would appear that the thermal decomposition of pernitric acid ([R25]) might be one of the pivotal reactions of this sequence. This reaction can rapidly return  $\text{HO}_2$  to the  $\text{HO}_x$  reservoir and yet the rate coefficient for this process,  $k_{25}$ , has one of the largest uncertainties associated with it at low temperatures (DeMore et al., 1997). This uncertainty has been estimated to be as large as a factor of 10 for SP summertime conditions. Sensitivity tests, however, have suggested that  $\text{HO}_x$  levels are relatively insensitive to the value of  $k_{25}$ . For a factor of 10 reduction in  $k_{25}$ , calculated  $\text{HO}_x$  levels decreased by 10% or less. Increasing  $k_{25}$  by the same factor, however, led to  $\text{HO}_x$  increases of up to 60%. Based on an analysis of  $\text{NO}_x$  and  $\text{HO}_2\text{NO}_2$  observations, Slusher et al. (2002) suggested that the upper limit on the uncertainty of  $k_{25}$  should be no more than a factor of 3.3. In this case, the variation of  $\text{HO}_x$  driven by  $k_{25}$  would be less than 20%.

Heterogeneous losses of  $\text{HO}_x$  may also be quite important at SP (Chen et al., 2001b). During ISCAT 1998, observations suggested significant  $\text{HO}_2$  scavenging frozen fog droplets on two occasions. A similar event occurred over the time period of 12–13 December during ISCAT 2000. At this time, the SP meteorological station recorded nearly 24 h of frozen fog and fog/misty conditions with visibility dropping from over 10 to  $\sim 1$  km. On this occasion, the NO level also dropped from an average of 175 pptv to less than 10 pptv. The photolysis rates  $j\text{O}^1(D)$  and  $j(\text{NO}_2)$  decreased by a factor of 1.3 and 1.5, respectively. The levels of  $\text{CH}_2\text{O}$  reduced from  $\sim 140$  to 35 pptv; while the  $\text{H}_2\text{O}_2$  decreased from  $\sim 250$  to  $\sim 75$  pptv. And finally, OH values dropped from an average of  $3 \times 10^6$ – $1.3 \times 10^5 \text{ molec cm}^{-3}$ . Unfortunately, there were no  $\text{HO}_2$  values recorded during this time period.

As in ISCAT 1998, we believe that the cited shift in OH during ISCAT 2000 was caused by two factors: (1) a decrease in precursors, i.e., NO and, to a much lesser extent,  $\text{H}_2\text{O}_2$  and  $\text{CH}_2\text{O}$  and (2) scavenging of  $\text{HO}_2$  by fog droplets. The impact from dropping NO levels was addressed earlier in this text in Section 3.1 and is directly tied to the recycling of OH through reaction [R4]. Regarding the impact of fog droplets on  $\text{HO}_x$ , there have been field observations showing large  $\text{HO}_x$  decreases in clouds (e.g., Mauldin et al., 1998). Model sensitivity calculations showed a significant reduction in OH due to lower values of NO; however, these values

were still nearly a factor of 7 times higher than the observations for the time period corresponding to the on-set of ice-fog. Chen et al. (2001b) previously estimated a median value for heterogeneous loss of  $\text{HO}_2$  of  $9 \times 10^{-3} \text{ s}^{-1}$ . This estimate was derived from a fog droplet size range of 5–10  $\mu\text{m}$  having a number density of 5–15  $\text{cm}^{-3}$ . Use of this  $\text{HO}_2$  loss rate coefficient led to a decrease by factor of 3 for OH and a factor of 8 for  $\text{HO}_2$ . Although the model OH remains to be more than a factor of two higher than the observations, the difference is within the bounds of the combined uncertainty for both model and observations. Even further increase the  $\text{HO}_2$  loss rate to the maximum value, the model OH decrease would be less than 20% while  $\text{HO}_2$  reduction is proportional to its loss rate increase. This is because the  $\text{HO}_2$  is already so low that the contribution from OH secondary formation ( $\text{HO}_2$  reaction) is nearly negligible. Although addition of heterogeneous loss to the model has not reproduced the observations of OH, it is evident that the  $\text{HO}_2$  heterogeneous loss may be quite important and requires further clarifications. The future study should include in-situ simultaneous observations of both OH and  $\text{HO}_2$  as well as the number size distribution of SP fog droplets.

### 3.4. Assessment of $\text{HO}_x$ budget

Fig. 5 summarizes the important SP  $\text{HO}_x$  photochemical processes. As discussed earlier in the text, the snow emissions of  $\text{H}_2\text{O}_2$  and  $\text{CH}_2\text{O}$  must be included as  $\text{HO}_x$  sources not only in Arctic sites (e.g., Hutterli et al., 2001) but also in SP and possibly in other snow covered areas. Considering the sources and sinks shown in the figure, a  $\text{HO}_x$  budget analysis is carried out using the mid NO level (i.e., 89 pptv) condition as defined earlier in Section 3.2. It was noted here that the best agreement between model predictions and observations was found around this NO level (e.g., see Figs. 2a and b).

Summarized in Fig. 6a are the major sources of SP  $\text{HO}_x$ . The largest source is that labeled as ‘Snow Emissions’. This source is made up of  $\text{HO}_x$  produced from the photolysis of snow released  $\text{CH}_2\text{O}$  and  $\text{H}_2\text{O}_2$ . They define  $\sim 32\%$  and  $14\%$  of the total  $\text{HO}_x$  source, respectively. Next in line are  $\text{CH}_4$  oxidation chemistry and  $\text{O}_3$  photolysis. Both of these contribute  $\sim 27\%$ . Of the total  $\text{CH}_2\text{O}$  contribution (snow +  $\text{CH}_4$  oxidation), 54% is from snow emissions and 46% comes from  $\text{CH}_4$  oxidation. Overall, therefore, snow emissions define the single largest source of SP  $\text{HO}_x$  (i.e. 46%). A comparison with the standard model output reveals that snow emissions lead to a factor of 2.3 increase in the total  $\text{HO}_x$  formation rate (vs. a factor 1.8 of in  $\text{HO}_x$  abundance). Similar results have been shown in the Arctic studies carried out in Alert, Canada and Summit Greenland (Yang et al., 2002; Hutterli et al., 2001). Finally, we would like to note that our sensitivity

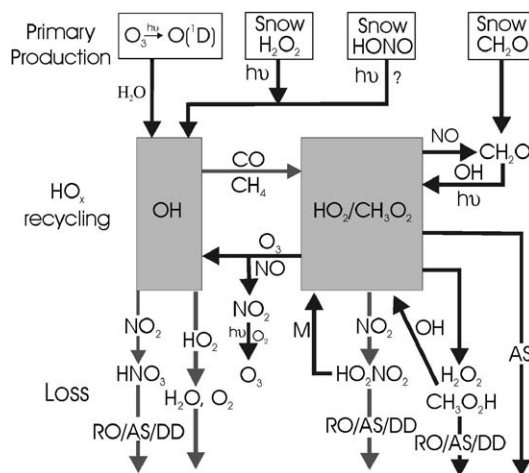


Fig. 5. Simplified  $\text{HO}_x$ - $\text{NO}_x$ - $\text{CH}_4$  photochemical scheme reflecting SP summertime photochemistry. (Modified from Fig. 1. in Chen et al. (2001a, b).)

calculations suggest that for the case of zero deposition the snow emission would still make up 23% of the total  $\text{HO}_x$  production. In this case,  $\text{CH}_4$  oxidation would be the largest  $\text{HO}_x$  source, contributing 50%; while the remainder 27% is the contribution from the reaction of  $\text{O}(^1\text{D}) + \text{H}_2\text{O}$ .

Major SP  $\text{HO}_x$  sinks are summarized in Fig. 6b. As presented in Section 3.3, the largest of these is the loss of  $\text{HO}_2$  through the formation and subsequent deposition of  $\text{HO}_2\text{NO}_2$  ([R29]). In addition,  $\text{HO}_2\text{NO}_2$  can lead to further  $\text{HO}_x$  loss via its reaction with OH (e.g., [R28]). Together, these two  $\text{HO}_2\text{NO}_2$  related  $\text{HO}_x$  loss pathways define  $\sim 45\%$  of the total. The significant role of  $\text{HO}_2\text{NO}_2$  in removing SP  $\text{HO}_x$  reflects the fact that  $\text{HO}_2\text{NO}_2$  is reasonably stable due to low temperature and can be rapidly deposited to snow. The radical-radical reaction (i.e.,  $\text{OH} + \text{HO}_2$ , [R9]) contributes another 30%. The final contribution comes from the reaction of OH with  $\text{NO}_2$  to produce  $\text{HNO}_3$ , [R20], which then mainly undergoes deposition to the surface snow ([R23]). The latter process makes up the last 24% of the total  $\text{HO}_x$  sink. The above cited losses lead to an overall  $\text{HO}_x$  lifetime estimate of 5.8 min. By comparison, the lifetime estimated using the standard model is 6.8 min.

Significant differences exist in the estimated  $\text{HO}_x$  losses for ISCAT 2000 vs. ISCAT 1998. Chen et al. (2001a, b) suggested that the major  $\text{HO}_x$  loss (i.e., 62%) was through  $\text{HNO}_3$  reactions ([R23] and [R22]). In ISCAT 2000, however, the major  $\text{HO}_x$  loss pathway was shown to be through  $\text{HO}_2\text{NO}_2$  reactions. Furthermore, at the lower NO levels encountered in 2000 formation of  $\text{HO}_2\text{NO}_2$  ([R13]) is more efficient than that of  $\text{HNO}_3$



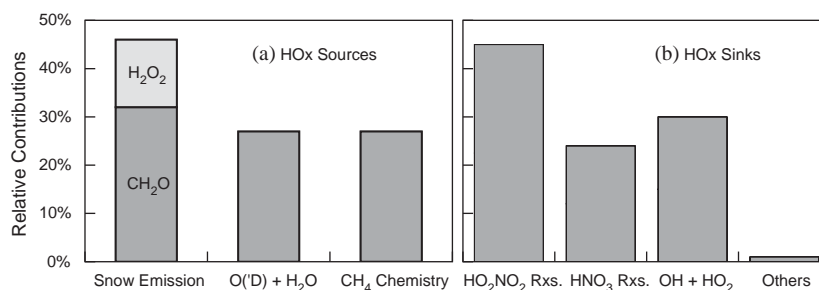


Fig. 6. HO<sub>x</sub> budget analysis for SP summertime Photochemistry: (a) sources, (b) sinks. This analysis is based on the use of the mid NO case at 89 pptv.

([R42]) because of higher HO<sub>2</sub> level. As shown in Figs. 1b and 2b, the HO<sub>2</sub> concentration rapidly decrease with increasing NO levels. A close examination of the model results revealed that the HO<sub>x</sub> loss through HO<sub>2</sub>NO<sub>2</sub> is more important when NO levels are lower than ~120 pptv. On the other hand, at a given NO level, our sensitivity test shows the HO<sub>2</sub> level is a strong function of the HO<sub>x</sub> primary production (e.g., [R2]).

### 3.5. Implications to SP surface ozone

Crawford et al. (2001) has shown strong evidence suggesting surface photochemistry can play a significant role in modifying the SP surface ozone seasonal trend and generate late Spring/early Summer perturbations in O<sub>3</sub> level that exceeded the Winter maximum levels. These authors reported a median model estimated net ozone production rate of 2.8 ppbv day<sup>-1</sup>. This production rate is equivalent to nearly 10% of average SP surface ozone concentration per day. Based on the observations from 2000, we have estimated the median net ozone production rate ( $P(O_3)$ ) of 4.2 ppbv day<sup>-1</sup> or nearly 13% per day. As shown in Fig. 7, the  $P(O_3)$  is a strong non-linear function of NO level. The peak  $P(O_3)$  value of ~6.5 ppv day<sup>-1</sup> situates around 160 pptv of NO and the inner quartile range was estimated to be from 3.2 to 4.8 ppbv day<sup>-1</sup>. The higher values in 2000 can mainly be attributed to two factors: observed NO range and extra HO<sub>x</sub> sources from snow emission of H<sub>2</sub>O<sub>2</sub> and CH<sub>2</sub>O. Recall the observed NO median for the 1998 study was 225 pptv (Davis et al., 2001) and the median derived from observations of 2000 is only 89 pptv. As shown by Crawford et al. (2001), the net ozone production rate has fallen to less than half of the peak value at 225 pptv of NO. By contrast, well over 73% of model runs for 2000 data give  $P(O_3)$  values larger than the half of the peak value of ~6.5 ppbv day<sup>-1</sup>. The non-monotonic relation between  $P(O_3)$  and NO has been discussed by Crawford et al. (2001). These authors have shown the linkage the intensity of photochemistry with the magnitude of  $P(O_3)$ . This can be also seen here by

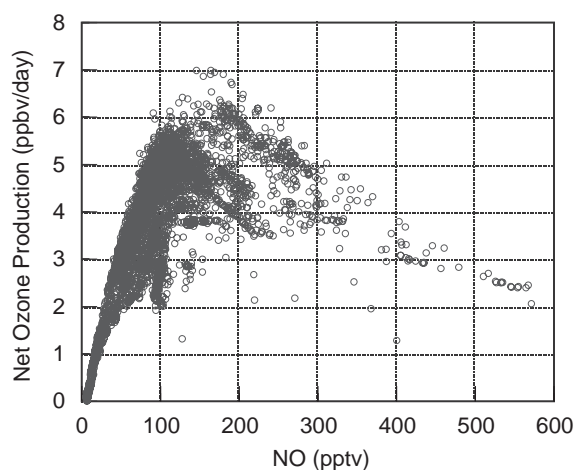


Fig. 7. Model calculated net O<sub>3</sub> production vs. observed NO for SP during ISCAT 2000.

comparing the Figs. 1 and 2 with Fig. 7. In fact, the  $P(O_3)$  and model predicted OH is highly correlated with an  $R^2$  value of 0.97. This is because both  $P(O_3)$  and OH levels are largely controlled by the reaction of HO<sub>2</sub> with NO.

Generally, the  $P(O_3)$  trend closely mimics that of the gross ozone production rate ( $F(O_3)$ ). This reflects the fact that the photochemical ozone destruction rate ( $D(O_3)$ ), on average, is less than 18% of  $F(O_3)$  values. The major ozone production channel is the reaction of HO<sub>2</sub>+NO, contributing nearly 80% of total. The remainder is through the CH<sub>3</sub>O<sub>2</sub>+NO reaction. The two largest O<sub>3</sub> destruction pathways are the reactions of OH+O<sub>3</sub> and HO<sub>2</sub>+O<sub>3</sub>, constituting ~46% and ~23% of the total, respectively. The relative importance of these two processes can be understood by the low HO<sub>2</sub>/OH ratio of ~16 and the enhanced reaction rate coefficient difference of a factor of 33, resulting from the SP environmental conditions characterized by low temperature and high NO levels. The reaction of O(<sup>1</sup>D)+H<sub>2</sub>O makes up a mere 12% due to the dryness

of SP. The remaining 18% of ozone loss is through a sequence of reactions starting from  $\text{NO} + \text{O}_3$  and followed by  $\text{NO}_2 + \text{OH}$ .

#### 4. Summary and conclusions

The OH levels recorded in ISCAT 2000 now place the average 24 h oxidizing capacity of near surface air at SP to be larger than that in the tropical marine BL. The current analysis of SP  $\text{HO}_x$  chemistry has provided strong evidence that SP  $\text{HO}_x$  levels not only have a strong dependence on snow emissions of NO but also on emissions of  $\text{CH}_2\text{O}$  and  $\text{H}_2\text{O}_2$ . Both compounds were found to be present at SP at levels much higher than those predicted based on gas phase photochemistry alone. The model analysis suggests that the observations of HONO are inconsistent with both the observations of  $\text{HO}_x$  and NO. The difference between observations and model predications far exceeds the limits defined by the combined uncertainties for the model and observations. By contrast, constraining the model with observed values of  $\text{CH}_2\text{O}$  and  $\text{H}_2\text{O}_2$  leads to model predicted  $\text{HO}_x$  levels that are well within the aforementioned uncertainties. Our results related to HONO would appear to be in conflict with those found at Summit Greenland and at other Arctic polar sites where HONO has been identified as the major OH source. On the other hand, it must be recognized that no direct observations of OH were available at these Arctic sites to test their conclusions.

A  $\text{HO}_x$  budget analysis has revealed that snow emissions of  $\text{CH}_2\text{O}$  and  $\text{H}_2\text{O}_2$  may constitute the single largest  $\text{HO}_x$  source at SP. The total contribution is estimated at 46%, 32% of which could be assigned to  $\text{CH}_2\text{O}$  and 14% to  $\text{H}_2\text{O}_2$ . The other important sources are identified as  $\text{CH}_4$  oxidation chemistry and  $\text{O}_3$  photolysis (i.e.,  $\text{O}(^1D) + \text{H}_2\text{O}$ ), each contributing  $\sim 27\%$ . The greater efficiency of  $\text{CH}_2\text{O}$  in its influence on  $\text{HO}_x$  levels primarily reflects the five times higher photolysis rate of  $\text{CH}_2\text{O}$ . Over 93% of the impact from  $\text{H}_2\text{O}_2$  is estimated to come from snow emissions of this species. In contrast, only 60% of the impact from  $\text{CH}_2\text{O}$  is from snow emissions, with the remainder coming from  $\text{CH}_4$  oxidation chemistry.

The analysis of SP  $\text{HO}_x$  sinks indicates that the largest sink is through the reaction [R24],  $\text{HO}_2 + \text{NO}_2$  (45%), followed by  $\text{HO}_2\text{NO}_2$  dry deposition and reaction with OH ([R27] and [R26]). The second largest sink involves the radical–radical reaction,  $\text{OH} + \text{HO}_2$  (e.g., 30% of the total). Loss of  $\text{HO}_x$  through  $\text{HNO}_3$  contributes  $\sim 24\%$ . The relative importance of  $\text{HO}_x$  loss through  $\text{HO}_2\text{NO}_2$  vs.  $\text{HNO}_3$  is primarily dictated by the ambient NO level.

It is evident that additional polar studies of  $\text{HO}_x$  chemistry will be required. Having available simultaneous observations of  $\text{HO}_2$  and OH will be a critical

need. Obviously, a resolution of the importance of HONO as a source of OH and  $\text{NO}_x$  will also be critical. The latter will require new specific measurement techniques for HONO as well as a reassessment of model  $\text{HO}_x$  sink processes.

#### Acknowledgements

The authors would like to acknowledge that this research is partially supported by the NSF office of Polar programs and the Division of Atmospheric Chemistry through Grant #OPP-9725465. The authors would also like to thank NOAA's CMDL group for making available SP  $\text{O}_3$ , CO, and meteorological data and the Raytheon staff for helping us make this field mission a successful one. Of particular significance are the contributions from Mr. Dana Hrubec.

#### References

- Chameides, W.L., Davis, D.D., 1982. Chemistry in the troposphere. *Chemical and Engineering News* 60, 38–52.
- Chamedies, W.L., Tan, A., 1981. The two-dimensional diagnostic model for tropospheric OH: an uncertainty analysis. *Journal of Geophysical Research* 86, 5209–5223.
- Chen, G., et al., 2001a. An assessment of  $\text{HO}_x$  chemistry in the tropical Pacific boundary layer: comparison of model simulations with observations recorded during PEM tropics A. *Journal of Atmospheric Chemistry* 38, 317–344.
- Chen, G., et al., 2001b. An investigation of South Pole  $\text{HO}_x$  chemistry: comparison of model results with ISCAT observations. *Geophysical Research Letters* 28, 3633–3636.
- Crawford, J., et al., 1999. Assessment of upper tropospheric  $\text{HO}_x$  sources over the tropical Pacific based on NASA GTE/PEM data: net effect on  $\text{HO}_x$  and other photochemical parameters. *Journal of Geophysical Research* 104, 16255–16273.
- Crawford, J., et al., 2001. Evidence for photochemical production of ozone at the South Pole surface. *Geophysical Research Letters* 28, 3641–3644.
- Davis, D., et al., 2001. Unexpected high levels of NO measured at South Pole. *Geophysical Research Letters* 28, 3625–3628.
- Davis, D., Eisele, F., Chen, G., et al., 2004a. Overview of ISCAT 2000. *Atmospheric Environment*, 2004, this issue, doi:10.1016/j.atmosenv.2004.05.037.
- Davis, D., et al., 2004b. South Pole  $\text{NO}_x$  chemistry: an assessment of factors controlling its variability and absolute levels. *Atmospheric Environment*, 2004, this issue, doi:10.1016/j.atmosenv.2004.04.039.
- DeMore, W.B., et al., 1997. Chemical kinetics and photochemical data for use in stratospheric modeling, evaluation number 12. Technical Report JPL Publication 97-4, NASA Jet Propulsion Laboratory.
- Dibb, J.E., Arsenault, M., Peterson, M.C., Honrath, R.E., 2002. Fast nitrogen oxide photochemistry in Summit, Greenland snow. *Atmospheric Environment* 36 (15–16), 2501–2511.

- Dibb, J.E., Huey, L.G., Slusher, D.L., Tanner, D.J., 2004. Soluble reactive nitrogen oxides at South Pole during ISCAT 2000. *Atmospheric Environment*, 2004, this issue, doi:10.1016/j.atmosenv.2003.01.001.
- Hutterli, M.A., Rothlisberger, R., Bales, R.C., 1999. Atmosphere-to-snow-to-firn transfer studies of HCHO at Summit, Greenland. *Geophysical Research Letters* 26, 1691–1694.
- Hutterli, M.A., McConnell, J.R., Stewart, R.W., Jacobi, H.-W., Bales, R.C., 2001. Impact of temperature-driven cycling of hydrogen peroxide (H<sub>2</sub>O<sub>2</sub>) between air and snow on the planetary boundary layer. *Journal of Geophysical Research* 106 (D14), 15395–15404.
- Hutterli, M.A., Bales, R.C., McConnell, J.R., Stewart, R.W., 2002. HCHO in Antarctic snow: preservation in ice cores and air–snow exchange. *Geophysical Research Letter* 29 (8), 10.1029/2001GL014256.
- Hutterli, M., et al., 2004. Formaldehyde and hydrogen peroxide in air, snow, and interstitial air at South Pole. *Atmospheric Environment*, 2004, this issue, doi:10.1016/j.atmosenv.2004.06.003.
- Jaegle, L., et al., 2000. Photochemistry of HO<sub>x</sub> in the upper troposphere at northern midlatitudes. *Journal of Geophysical Research–Atmospheres* 105, 3877–3892.
- Jaegle, L., et al., 2001. Chemistry of HO<sub>x</sub> radicals in the upper troposphere. *Atmospheric Environment* 35, 469–489.
- Levy, H., 1974. Photochemistry of the troposphere. *Advances in Photochemistry*, Vol. 9. Wiley, New York, pp. 369–524.
- Logan, J., et al., 1981. Tropospheric chemistry: a global perspective. *Journal of Geophysical Research* 86, 7210–7254.
- Lurmann, F.W., Lloyd, A.C., Atkinson, R., 1986. A chemical mechanism for use in long-range transport/acid deposition computer modeling. *Journal of Geophysical Research* 91, 10905–10936.
- Mauldin, R.L., Frost, G.J., Chen, G., Tanner, D.J., Prevot, A.S.H., Davis, D.D., Eisele, F.L., 1998. OH Measurements during the first aerosol Characterization Experiment (ACE 1): observations and model comparisons. *Journal of Geophysical Research* 103, 16713–16729.
- Mauldin, R.L., Tanner, D.J., Eisele, F.L., 1999. Measurements of OH during PEM-Tropics A. *Journal of Geophysical Research–Atmospheres* 104, 5817–5827.
- Mauldin, R.L., et al., 2001. Measurements of OH aboard the NASA P-3 during PEM-Tropics B. *Journal of Geophysical Research–Atmospheres* 106, 32657–32666.
- Mauldin, R.L., et al., 2004. Measurement of OH, HO<sub>2</sub>/RO<sub>2</sub>, H<sub>2</sub>SO<sub>4</sub>, and MSA during ISCAT 2000. *Atmospheric Environment*, 2004, this issue, doi:10.1016/j.atmosenv.2004.06.031.
- McConnell, J.R., et al., 1997. Physically based modeling of atmosphere-to-snow-to-firn transfer of hydrogen peroxide at South Pole. *Journal of Geophysical Research* 103, 10561–10570.
- Olson, J.R., et al., 2001. Seasonal differences in the photochemistry of the South Pacific: a comparison of observations and model results from PEM-Tropics A and B. *Journal of Geophysical Research–Atmospheres* 106, 32749–32766.
- Oncley, S., Buhr, M., Lenschow, D., Davis, D., Semmer, S., 2004. Observations of summertime NO fluxes and boundary-layer height at the South Pole using scalar similarity. *Atmospheric Environment*, 2004, this issue, doi:10.1016/j.atmosenv.2004.05.053.
- Slusher, D.L., et al., 2002. Measurements of Peroxy Acid at the South Pole During ISCAT 2000. *Geophysical Research Letters* 29 (21), 10.1029/2002GL015703.
- Sumner, A., Shepson, P., 1999. Snowpack production of formaldehyde and its impact on the Arctic Troposphere. *Nature* 398, 230–233.
- Sumner, A.L., et al., 2002. Atmospheric chemistry of formaldehyde in the Arctic troposphere at Polar Sunrise, and the influence of the snowpack. *Atmospheric Environment* 36 (15–16), 2553–2562.
- Tan, D., et al., 1998. In situ measurements of HO<sub>x</sub> in aircraft exhaust plumes and contrails during SUCCESS. *Geophysical Research Letters* 25, 1721–1724.
- Tan, D., et al., 2001. HO<sub>x</sub> budgets in a deciduous forest: results from the prophet summer 1998 campaign. *Journal of Geophysical Research–Atmospheres* 106, 24407–24427.
- Thompson, A.M., 1992. The oxidizing capacity of the Earth's atmosphere—probable past and future changes. *Science* 256, 1157–1165.
- Wang, Y.H., et al., 2001. Factors controlling tropospheric O<sub>3</sub>, OH, NO<sub>x</sub> and SO<sub>2</sub> over the tropical Pacific during PEM-Tropics B. *Journal of Geophysical Research–Atmospheres* 106, 32733–32747.
- Yang, J., et al., 2002. Impacts of snowpack emissions on deduced levels of OH and peroxy radicals at Summit, Greenland 15–16, 2523–2534.
- Zhou, X., et al., 2001. Snowpack photochemical production of HONO: a major source of OH in the Arctic boundary layer in springtime. *Geophysical Research Letters* 28, 4087–4090.